JACS
JOURNAL OF THE AMERICAN CHEMICAL SOCIETY

Article

Addressing Kinase-Independent Functions of Fak via PROTAC-mediated Degradation

Philipp M. Cromm, Kusal Samarasinghe, John Hines, and Craig M Crews

J. Am. Chem. Soc., **Just Accepted Manuscript** • DOI: 10.1021/jacs.8b08008 • Publication Date (Web): 16 Nov 2018

ACS Publications

is published by the American Chemical Society. 1155 Sixteenth Street N.W., Washington, DC 20036

Addressing Kinase-Independent Functions of Fak via PROTAC-mediated Degradation

*Philipp M. Cromm[1] Kusal T.G. Samarasinghe[1], John Hines[1] and Craig M. Crews[1,2,3]**

[1] Department of Molecular, Cellular & Developmental Biology, Yale University, New Haven, CT 06511, USA.

[2] Department of Chemistry, Yale University, New Haven, CT 06511, USA.

[3] Department of Pharmacology, Yale University, New Haven, CT 06511, USA.

* To whom correspondence should be addressed.

E-mail: craig.crews@yale.edu

Abstract

Enzymatic inhibition has proven to be a successful modality for the development of many small molecule drugs. In recent years, small molecule-induced protein degradation has emerged as an orthogonal therapeutic strategy that has the potential to expand the druggable target space. Focal adhesion kinase (Fak) is a key player in tumor invasion and metastasis, acting simultaneously as a kinase and a scaffold for several signaling proteins. While previous efforts to modulate Fak activity were limited to kinase inhibitors with low success in clinical studies, protein degradation offers a possibility to simultaneously block Fak's kinase signaling and scaffolding capabilities. Here, we report the development of a selective and potent Fak degrader, **PROTAC-3**, which outperforms a clinical candidate, defactinib, with respect to Fak activation as well as Fak-mediated cell migration and invasion. These results underline the potential that PROTACs offer in expanding the druggable space and controlling protein functions that are not easily addressed by traditional small molecule therapeutics.

TOC graphic

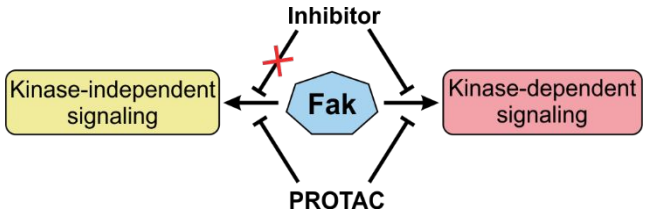

Introduction

Focal adhesion kinase (Fak) is a cytoplasmic tyrosine kinase that controls many aspects of tumor growth (e.g., invasion, metastasis and angiogenesis) through kinase-dependent and kinase-independent mechanisms.[1–3] In addition to its central kinase domain, Fak is comprised of three additional domains, a N-terminal four-point-one, ezrin, radixin, moesin (FERM) domain, a proline-rich region and a focal adhesion targeting (FAT) C-terminal domain, all of which mediate Fak kinase-independent signaling.[4,5] Through its scaffolding domains Fak is involved in the formation of large signaling complexes primarily at the plasma membrane.[1,5,6] Fak activation can be triggered upon engaging membrane proteins such as integrins, resulting in Fak FERM domain displacement and subsequent autophosphorylation at Y397. Phosphorylation at Y397 creates a binding site for Src-family kinases, which phosphorylate the kinase domain activation loop (Y576 and Y577) leading to full Fak activation and formation of an activated Fak-Src complex. Increased Fak expression and activity can be found in primary and metastatic cancers of many tissues and is often associated with poor overall patient survival.[2,7] This has rendered Fak an interesting target for drug discovery with multiple compounds in clinical trials.[1] Additionally, Fak activity has been associated with $CD8^+$ T cell exhaustion and is believed to be a valuable target for cancer immunotherapy.[8,9] However, the current medicinal chemistry toolbox limits the development of chemical entities to Fak kinase inhibitors, thus ignoring the Fak scaffolding role. While some of these compounds have proven effective in preclinical studies, clinical success has yet to be observed.[1,10] Thus far, the leading Fak inhibitor, defactinib (Verastem VS-6063), failed its initial clinical trial targeting malignant pleural mesothelioma stem cells although it is further being evaluated in combination with the anti-PD-1 immune checkpoint antibody, avelumab, for advanced ovarian cancer. Nevertheless, many essential functions mediated by the Fak scaffolding role are still beyond the reach of any kinase inhibitor.[3,11,12] To overcome the mechanistic shortcomings of Fak kinase inhibitors, we designed highly selective, low nanomolar Fak degraders. The most promising degrader, **PROTAC-3**, significantly exceeds the effects of defactinib on Fak signaling as well as on cell migration and invasion in human triple negative breast cancer (TNBC) cells.

Due to the mode of action (MOA)-based limitations of Fak kinase inhibitors we utilized our lab's Proteolysis Targeting Chimera (PROTAC) approach, which allows deliberate degradation of target proteins using the cells' own degradation machinery, to address Fak kinase-independent functions.[13–15] PROTACs are bifunctional molecules combining a E3 ligase recruiting element with a protein of interest (POI)-targeting warhead to facilitate subsequent POI ubiquitination and degradation by the ubiquitin proteasome system.[16,17] Several different E3 ligases have been used by PROTACs to degrade recruited target proteins. These include β-TrCP, MDM2, and IAP.[16,18–20] In addition, the two E2 ligases von Hippel-Lindau (VHL) and cereblon (CRBN), have been extensively used for PROTAC-mediated protein degradation.[21–25] VHL can be recruited by a rationally designed peptidomimetic based on an essential hydroxyproline pharmacophore. As

stereochemistry on the hydroxyproline pharmacophore is crucial for VHL binding, a degradation-incompetent diastereomer can be synthesized by flipping the stereo center at the hydroxyproline.[26–28] For CRBN-mediated protein degradation the thalidomide family of CRBN binding immunomodulary drugs (IMiDs) have been harnessed.[23]

Results

PROTAC design and efficacy.

Fak-degrading PROTACs were designed based on the most advanced clinical Fak inhibitor, defactinib (Figure 1A). Guided by previous SAR studies, the left part of the molecule was chosen for linker incorporation.[29] Although the N-methyl benzamide of defactinib presents a synthetically amenable handle for linker incorporation via amide bond formation it was replaced by 4-aminophenol to facilitate linker attachment via the phenol. This structural adjustment was made to minimize the number of amides within the final molecule and thus improve cellular permeability. From the previous reported SAR it was evident that an ether linkage at this position would be well tolerated.[29] Due to synthetic challenges, the 2,3-substituted pyrazine was replaced by a 1,3-substituted benzyl that was previously reported to inhibit Fak with similar potency.[29] A set of six different linkers that vary in length and composition was attached to the modified defactinib warhead (Table 1, Supplementary Figure S24). Coupling these different linkers with the reported VHL ligand yielded **PROTACs 1-6** (Table 1, Supplementary Figure S25). Based on the inhibition and degradation data, the diastereomeric **PROTAC-7** was synthesized as a negative control for **PROTAC-3**. **PROTACs 8-10** were synthesized based on the linker composition of **PROTACs 4-6**, yet contain thalidomide as the E3 ligase recruiting element. Half-maximal inhibitory concentrations (IC_{50}) as well as half-maximal degradation concentrations (DC_{50}) and a degradation maximum (D_{max}) were calculated for **PROTACs 1-10** and defactinib. As expected, the optimized Fak inhibitor defactinib displays the most potent IC_{50} value (3.9 nM) of all tested compounds. Linker addition and coupling of the E3 recruiting element to this inhibitor does not have a major effect on Fak inhibition and no general trend was observed. All PROTACs inhibit Fak kinase activity with low nanomolar IC_{50}s between 4.7 nM and 14.5 nM (Table 1, Supplementary Figures S1). However, as already observed in previous studies, inhibition and degradation do not always correlate.[30] For example, the best Fak-inhibiting PROTAC, **PROTAC-9,** is one of the least potent degraders (DC_{50} 26.7 nM). On the contrary, **PROTAC-4** combines the least potent IC_{50} (14.5 nM) with the second most potent DC_{50} (4.0 nM). Inversion of the hydroxyproline stereo center on **PROTAC-7** (IC_{50} = 11.2 nM) results in a minimal loss of potency compared to its diastereomer **PROTAC-3** (IC_{50} = 6.5 nM). The maximum degradation efficacy (D_{max}) for most PROTACs is at the limit of detection (99%) (Supplementary Figures S3-S8); only the two PROTACs containing the longest linkers **PROTAC-6** and **PROTAC-10** show slightly reduced D_{max} of 91% and 87%, respectively. As expected, the negative control molecules, defactinib and the non VHL-binding diastereomer **PROTAC-7** induce no Fak degradation. As

a general trend, VHL-recruiting **PROTACs 1-6** appear to be more effective degraders than their CRBN–recruiting analogs **PROTACs 8-10**. In addition, linkers that are too long (**PROTACs 5-6**) or too short (**PROTAC-1**) yield less effective PROTACs with DC_{50}s of 20.8 nM, 48.1 nM and 23.2 nM, respectively. A three-carbon linkage on the VHL ligand appears to be preferred over a two-carbon linkage: **PROTAC-3** and **PROTAC-4** display almost identical DC_{50} values of 3.0 nM and 4.0 nM, respectively, combined with an excellent D_{max} of 99%, whereas **PROTAC-2** is slightly less potent with a DC_{50} of 7.6 nM. As **PROTAC-3** shows very efficient Fak degradation (Figure 1 B), has the slightly better DC_{50} and displays a stronger suppression of p-Fak(Y397) levels (Supplementary Figures S9 & S10) it was selected for all further characterization.

To assess the target selectivity of **PROTAC-3** over a large panel of different kinases, a DiscoverX KINOMEscan was performed. KINOMEscan measures compound binding to individual kinases via the compound's ability to compete/displace the kinases from an immobilized support that non-selectively binds kinase active sites (Supplementary Figure S2, Supplementary Table S1 & S2). Defactinib (1 μM) binds to 100 kinases such that less than 35% of the control (uncompeted) level of kinase remain attached to the support. However, **PROTAC-3** shows highly increased selectivity as it binds only 20 kinases to a comparable extent under identical conditions (Figure 1C, Supplementary Figure S2, Supplementary Table S1 & S2). Surprisingly, Fak is the only kinase bound by **PROTAC-3** with less than 1% of control remaining, whereas defactinib binds a total of 9 kinases to this extent (Supplementary Figure S2, Supplementary Table S1 & S2). It appears that the slight loss in inhibitory potency due to linker and VHL ligand attachment results in greater selectivity for **PROTAC-3**.

Table 1 Fak degrading PROTACs. Linker: n = number of carbons attached to E3 recruiting element, "-" = oxygen; m = number of carbons; n.d. = no degradation; n.l. = no linker; (a) Fak inhibition assays were performed by Reaction Biology Corp. in duplicates (Supplementary Figures S1,S2). Error = SD (b) Fak degradation was calculated from quantified western blots after 24 h serum-free treatment of PC3 cells in triplicates (Supplementary Figures S3-S8). Error = 1σ

entry	compound	linker (n-m)	IC_{50} (nM)[a]	D_{max} [b]	DC_{50} (nM)[b]
1	PROTAC-1	2-2	10.7 ± 0.3	99%	23.2 ± 8.1
2	PROTAC-2	2-3	14.7 ± 2.1	99%	7.6 ± 4.1
3	PROTAC-3	3-2	6.5 ± 0.5	99%	3.0 ± 1.5
4	PROTAC-4	3-3	14.5 ± 0.6	99%	4.0 ± 2.2
5	PROTAC-5	3-2-2	12.7 ± 0.1	99%	20.8 ± 9.1
6	PROTAC-6	3-2-2-2-2	6.1 ± 0.1	91%	48.1 ± 23.9
7	PROTAC-7	3-2	11.2 ± 1.9	0%	n.d.
8	PROTAC-8	3-3	11.3 ± 1.3	98%	8.2 ± 4.7
9	PROTAC-9	3-2-2	4.7 ± 0.3	99%	26.7 ± 14.8
10	PROTAC-10	3-2-2-2-2	9.7 ± 0.9	87%	< 10
11	defactinib	n.l.	3.9 ± 0.2	0%	n.d.

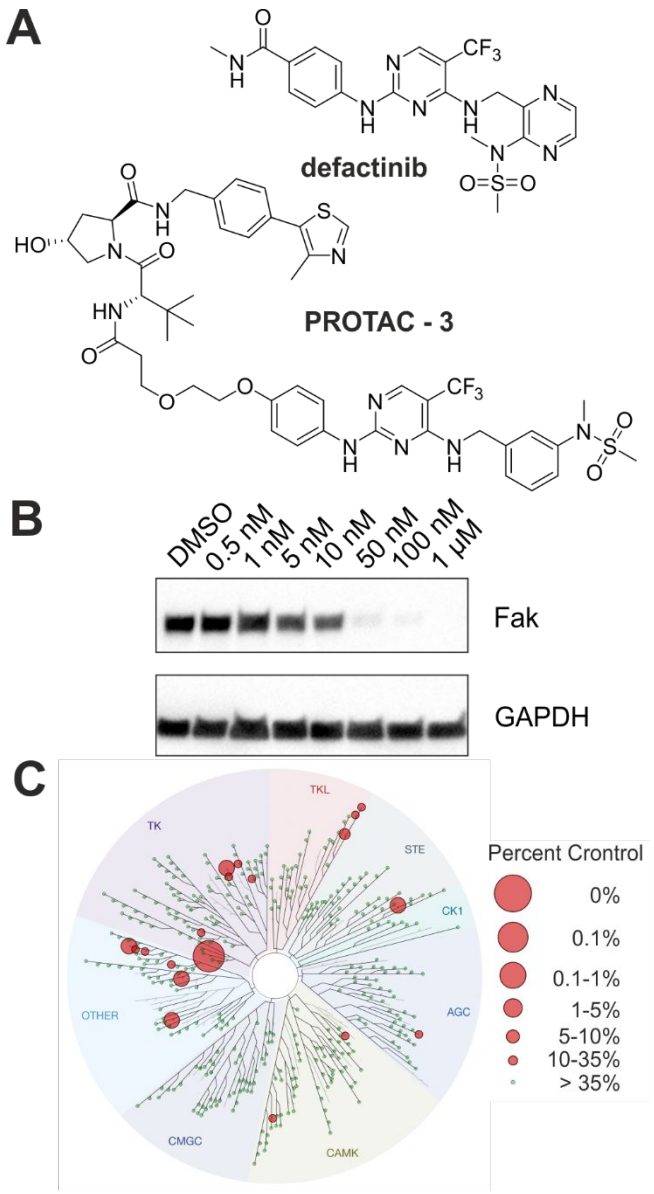

Figure 1 Fak degrading PROTACs. A) Chemical structures of the Fak kinase inhibitor defactinib and the most potent PROTAC, **PROTAC-3**. **B**) Dose response Fak degradation profile of **PROTAC-3** after 24 h serum-free incubation of PC3 cells. n = 3. **C**) Dendrogram of DiscoverX KINOMEscan results for **PROTAC-3** at 1 µM. Out of a panel of 403 different kinases **PROTAC-3** binds to only 20 kinases with less than 35% of control remaining measured by competitive binding.

Effects on downstream signaling.

To evaluate the benefits of Fak degradation over inhibition on downstream signaling, a head-to-head comparison between **PROTAC-3** and defactinib was performed (Figure 2, Supplementary Figure S11,S12). Human prostate tumor (PC3) cells were treated with increasing concentrations of **PROTAC-3** and defactinib and cellular effects were evaluated via western blotting for total Fak levels, Fak activity (autophosphorylation of Y397) as well as phosphorylation of two downstream targets of Fak: paxillin and

Akt. The cellular data obtained for defactinib's effect on Fak autophosphorylation is in agreement with previously reported results.[31] As already evident in Table 1, **PROTAC-3** induces highly efficient Fak degradation in a dose-dependent manner with only 34% total Fak remaining at 10 nM and 5% at 50 nM (Figure 2). Fak levels are undetectable at concentrations of 100 nM through 1 μM **PROTAC-3,** and slightly rebound at concentrations of 5 μM (10%) and 10 μM (27%) due to an observed hook effect.[32] In contrast, incubation with defactinib does not show any effect on Fak levels. Fak activation (p-Fak(Y397)) was significantly reduced at all **PROTAC-3** concentrations tested compared to DMSO: p-Fak levels of less than 5% were observed between 100 nM and 5 μM. Defactinib showed significantly reduced Fak activity only at concentrations above 100 nM, and at no concentration was defactinib able to outperform **PROTAC-3** with respect to p-Fak loss. The lowest level of p-Fak activity (26% remaining) was observed with 10 μM defactinib treatment, a concentration at which the inhibitor is predicted to show a high level of off-target activity (KINOMEscan). Paxillin, a downstream target of the Fak-Src complex, has been associated with cell migration.[1] Paxillin interacts with the FAT domain and reduced levels of Fak result in a reduction of p-paxillin.[33] **PROTAC-3** treatment above 50 nM is able to significantly reduce p-paxillin levels by as much as 85-90%. Defactinib, on the other hand, reduces p-paxillin levels by a maximum of only 62%, and then solely at the high concentration of 10 μM. Akt is a kinase that is tied to the Fak signaling cascade via PI3K,[1] but can be activated through other pathways as well. Consequently, the suppressive effect of **PROTAC-3** on p-Akt (S473) is not as pronounced as for paxillin and Fak, but nonetheless still significant at all treatment concentrations. A maximum p-Akt suppression of 93% is observed at 1 μM **PROTAC-3**. Conversely, defactinib shows no reduction of p-Akt at concentrations below 5 μM, and has a maximum reduction of p-Akt at 10 μM (88%). Judging by the high number of bound kinases at 1 μM (100 kinases, Supplementary Table S1, Supplementary Figure S2), it is very possible that the observed effects at 5 μM and 10 μM defactinib may be due to off-target binding. Evaluating the activation profile in Figure 2 it is clear that **PROTAC-3-**mediated Fak degradation has a more pronounced effect on the effector targets within the Fak signaling pathway compared to the clinical candidate defactinib. A similar differential can be observed when **PROTAC-3** is compared to its non-degrading diastereomer **PROTAC-7** (Supplementary Figures S11 & S12). These differences are the result of the distinct MOA that Fak degraders are able to provide compared to inhibitors.

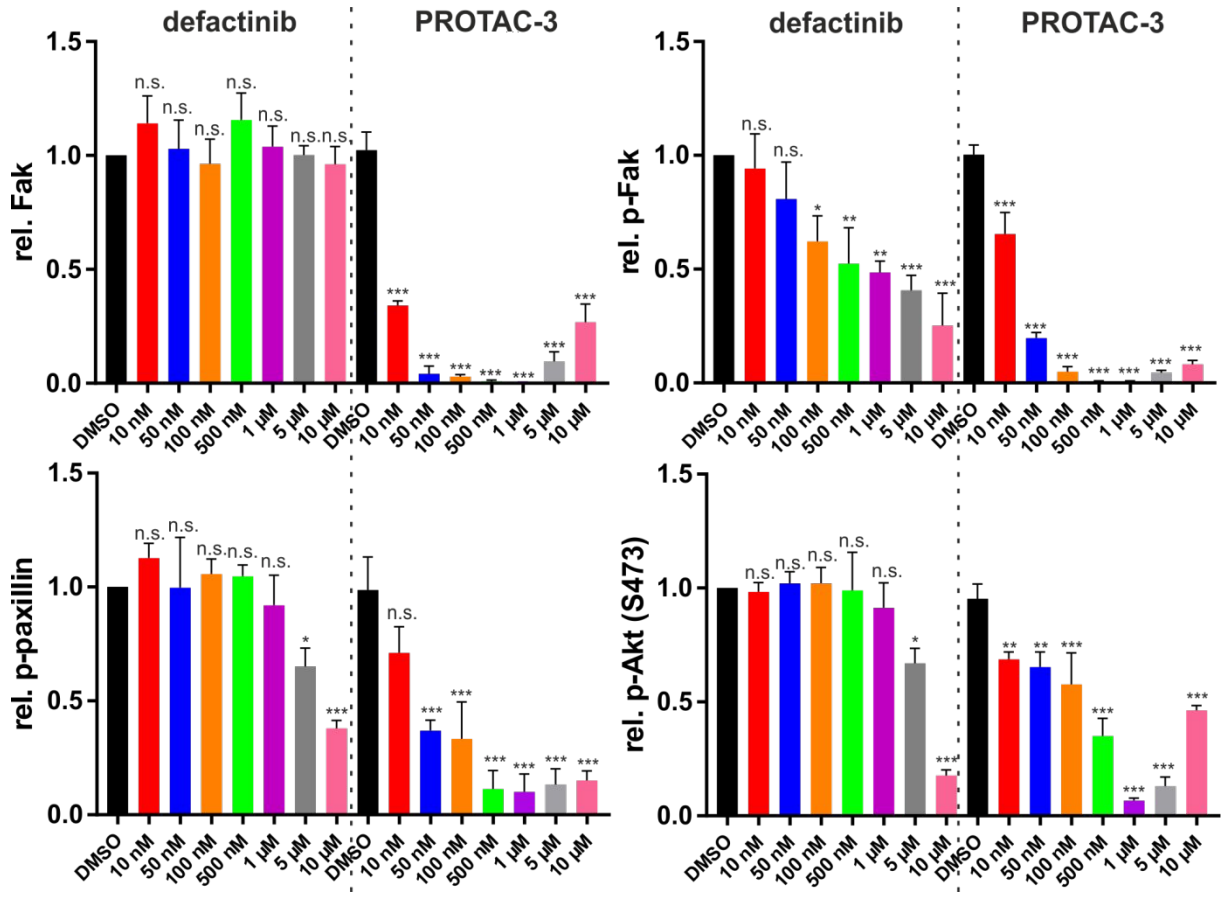

Figure 2 Fak signaling. Effects of Fak degradation (**PROTAC-3**) vs. Fak inhibition (defactinib) on total Fak levels, p-Fak(Y397), p-paxillin and p-Akt(S473). 24 h treatment in serum deprived PC3 cells. n.s. P value > 0.05; * P value <0.05; ** P value <0.01; *** P value < 0.001.

Cell migration and invasion.

Since Fak is a key regulator of cell motility, **PROTAC-3** was next evaluated for its effect on cell migration and invasion. Despite their previously described effects on Fak activation and signaling, **PROTAC-3** and defactinib do not affect cell viability or proliferation within four days (Supplementary Figures S21 & S22). Effects on cell migration were analyzed in a wound healing assay using the aggressive and invasive human TNBC cell line MDA-MB-231. **PROTAC-3** mediated Fak degradation in MDA-MB-231 cells was confirmed to be in the same range as for PC3 cells (Supplementary Figure S13). MDA-MB-231 cells were grown to confluency and a wound was created using a pipet tip. Wound closure was quantified after 24 h (Figure 3). While near-complete wound closure can be observed after 24 h in cultures treated with 50 nM defactinib or vehicle equivalent (DMSO), treatment with 50 nM **PROTAC-3** significantly impairs cell migration and results in a 53% reduction of wound healing. Moreover, treatment with 250 nM **PROTAC-3** further impairs wound closure by 70% (Figure 3B, Supplementary Figure S19), while 250 nM defactinib treatment results in a non-significant suppression of wound healing. Since PROTAC treatment did not affect

cell proliferation at the concentrations applied, the observed effects result from reduced migratory properties of cancer cells due to Fak degradation.

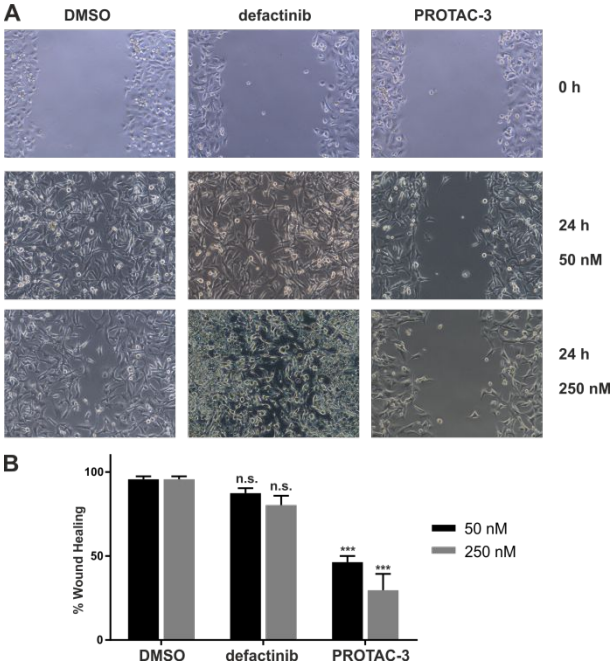

Figure 3 Wound healing assay. A) Effects of **PROTAC-3** and defactinib on wound healing of MDA-MB-231 cells. Wounded area was captured just after wound introduction and after 24h of treatment. **B)** Graphical representation of percent wound healing. n.s. P value > 0.05; ***P value < 0.001. n = 3.

To diminish the contribution of cell growth, a transwell cell invasion assay was performed (Figure 4). MDA-MB-231 cells were treated with **PROTAC-3** or defactinib at 100 nM and transwell migration was quantified after 24 h (Figure 4, Supplementary Figure S20). While **PROTAC-3** reduces MDA-MB-231 cell invasion by as much as 65%, no significant effect is observed for defactinib or DMSO. PROTAC treatment significantly impairs cell invasion compared to defactinib, underscoring the importance of Fak's scaffolding function in the context of cell migration and invasion. To attempt to pinpoint these observations to a molecular signaling event or specific downstream pathway, reverse phase protein array (RPPA) analysis was performed (Supplementary Table S3). RPPA results confirmed Fak degradation and reduced levels of p-Fak in **PROTAC-3** treated cells as well as reduced p-Fak levels after defactinib treatment. However, while the RPPA results did not reveal a specific pathway or scaffolding event responsible for the effects on migration and invasion, they gave grounds for speculation. Changes in protein levels observed by RPPA were validated by western blotting from cell lysates after incubation of MDA-MB-231 cells with varying concentrations of **PROTAC-3** and defactinib in the presence of serum (Supplementary Figures S14-S18). The most surprising effect was observed for the androgen receptor (AR) (Supplementary Figure S14). It has

been previously shown that extranuclear AR is involved in cell migration and forms a multiprotein complex comprised of filamin A/β-1 integrin/Fak/AR in NIH3T3 fibroblasts that facilitates Fak activation.[34,35] Based on the obtained RPPA data and verified from MDA-MB-231 cell lysates, a reduction of AR levels after **PROTAC-3** treatment was observed by western blotting (Supplementary Figure S14). As no similar effect on AR in defactinib-treated cells is observed, this suggests a specific involvement of extranuclear AR in Fak scaffold signaling and Fak mediated cell motility. Besides the changes in AR, reduced levels of p-Akt(S473) and p-Src(Y527) can be detected as well (Supplementary Figures S15 & S16). While p-Akt was characterized previously in PC3 cells (Figure 2), differences in p-Src(Y527) may arise from a disruption of the Fak-Src complex upon **PROTAC-3** mediated Fak degradation. The effect of defactinib on p-Src(Y527) at high concentrations might be based on off-target Src binding (Supplementary Table S2). Additionally, reduced phosphorylation of the S6 ribosomal protein (S6RP) in **PROTAC-3** treated cells can be observed while total S6RP levels remained unchanged. (Supplementary Figure S17 & S18). Phosphorylation of S6RP occurs via the Src-Fak-PI3K pathway and p-S6RP is required for the initiation of translation in response to cell growth and proliferation.[36,37]

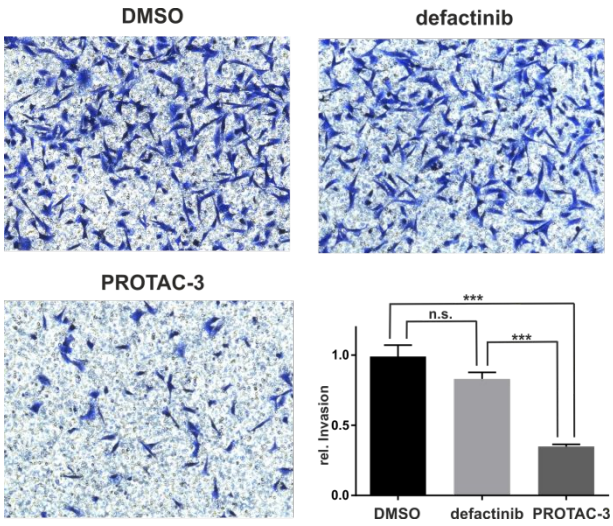

Figure 4 Transwell cell invasion. Invasion of MDA-MB-231 cell in response to **PROTAC-3** and defactinib treatment (100 nM) as determined by transwell assay. Cells were fixed, permeabilized and stained with crystal violet and examined under a light microscope. Invaded area was captured and cells quantified by counting after 24 h. Graphical representation of relative invasion. n.s. P value > 0.05; ***P value < 0.001. n = 3.

Discussion

Enzymes with a scaffolding function, e.g., Fak, which acts via kinase-dependent as well as kinase-independent signaling, pose particularly difficult challenges for traditional medicinal chemistry. The MOA of small molecule inhibitors inherently limits their field of use to enzymatic functions. To address the limitations posed by inhibitors, we have developed small molecule-like protein degraders that eliminate

targeted intracellular proteins by harnessing the cells' own proteolytic machinery. In this study, we developed PROTACs that effectively degrade Fak at low nanomolar concentration (Table 1) and outperform the clinical candidate defactinib in respect to Fak activation (autophosphorylation) and inhibition of downstream signaling (Figure 2). Additionally, **PROTAC-3** shows improved selectivity over defactinib (Figure1, Supplementary Table S1, Supplementary Figure S2) as it only binds to Fak with less than 1% of control compound remaining while defactinib binds a total of nine different kinases under identical conditions.

Inducing Fak degradation not only affects its kinase-dependent signaling activity but given the absence of Fak itself, Fak's kinase-independent signaling is impaired as well. The benefits of Fak degradation relative to Fak inhibition are especially prominent with respect to cell migration and invasion (Figure 3, 4). As Fak-mediated cell motility is mainly controlled by kinase-independent pathways Fak removal significantly hampers the ability of TNBC cells to migrate and invade. While defactinib shows non-significant effects in both assays, low nanomolar concertation of **PROTAC-3** are sufficient to significantly decrease wound healing and cell invasion of MDA-MB-231 cells. Our results highlight the advantages of protein degradation over protein inhibition for proteins like Fak and exemplify the differential biology that can result from different MOAs of various modalities.

Conclusion

Within the past decade, medicinal chemistry has increasingly faced the challenges of expanding the druggable space as more promising therapeutic targets are proposed that are yet out of reach of the traditional approaches.[38–42] Despite the success of many kinase inhibitors, which target an increasing range of kinases and therapeutic areas, some resistance mechanisms and protein targets remain inaccessible.[43,44] In this context, PROTACs are taking a leading role in advancing the druggable space as they facilitate effective degradation of a protein target using small molecule like chemical entities.[13–15] PROTACs not only allow the targeting of novel proteins that thus far out of reach, but they also allow targeting of additional functions of already established drug targets due to a different MOA. To our knowledge, **PROTAC-3** is the first degrader that outperforms an optimized kinase inhibitor and shows strong differential biology, due to its orthogonal MOA, allowing the PROTAC to modulate effects that are unobtainable with an inhibitor.

Experimental Methods

PROTAC Synthesis. Detailed information on PROTAC synthesis analytical data as well as supplementary data can be found in the Supporting Information.

Cell lines. PC3 cells were cultured in F12-K (Kaighn's Modification of Ham's F-12 Medium), supplemented with 10% FBS and 1% penicillin-streptomycin at 37 °C and 5% CO2. MDA-MB-231 cells were cultured in RPMI-1640 (ATCC), supplemented with 10% FBS and 1% penicillin-streptomycin at 37 °C and 5% CO_2.

Immunoblotting. If not indicated otherwise, cells were seeded and grown to 80% confluency and were treated with compound or control for 24 h. Subsequently, the growth media was removed and the cells lysed by the addition of lysis buffer (25 mM Tris, pH 7.4; 1% NP-40, 0.25% deoxycholate, 1 mM sodium vanadate, 10 mM sodium fluoride, 10 mM sodium pyrophosphate, 20 mM β-glycerophosphate and 1x cOmplete EDTA-free protease inhibitor cocktail (Roche)). After 20 min the mixture was spun down at 16,000 x g for 10 min at 4 °C to pellet insoluble materials. Protein concentration of supernatants were determined via BCA assay (Thermo Fisher) before addition of NuPAGE sample buffer containing 5% β–Me and boiling at 95 °C for 10 min. Equal amounts of protein were subjected to SDS-PAGE and subsequent electrophoretic transfer onto nitrocellulose membrane. Rabbit antibodies were purchased from Cell Signaling: Fak (3285), p-Fak (3283), p-Paxillin (2541), p-Akt (S473)(4060), GAPDH (2118), Androgen Receptor (5153), p-Src(Y527)(2105), p-S6RP (2215). Mouse antibodies were purchased from Cell Signaling: tubulin (3873), S6RP (2317). Secondary antibody α-rabbit (31460) or α-mouse (31444) was coupled to horseradish peroxidase and purchased from Thermo Fisher. Immunoblots were developed using enhanced chemiluminescence and visualized using a Bio-Rad Chemi-Doc MP Imaging System and quantitated with Image Lab v.5.2.1 software (Bio-Rad Laboratories). Data analysis and statistics was performed using Prism 7.0 (GraphPad).[45]

Cell Proliferation Assays. Cells were seeded in 96-well plates (2000 cell/well) and treated with PROTAC or control as indicated. At desired time points culture medium was supplemented with 330 mg/mL MTS (Promega) and 25 mM phenazine methosulfate (Sigma) and incubated at 37 °C. Mitochondrial reduction of MTS to the formazan derivative was monitored by measuring the medium's absorbance at 490 nm using a Wallac Victor2plater-eader (Perkin-Elmer Life Sciences). Data analysis and statistics was performed using Prism 7.0 (GraphPad).[45]

KinomeScan. The Kinase engagement assay (KINOMEscan) was performed by DiscoverX assessing binding abilities towards a set of 468 kinases. **PROTAC-3** and defactinib were screened at a concentration of 1 μM.

Kinase activity assay. Kinase activity assays were performed by Reaction Biology Corp.. Compounds were tested in 10-dose IC_{50} duplicate mode with a 3-fold serial dilution starting at 1 μM. Control compound, staurosporine, was tested in 10-dose IC_{50} mode with 4-fold serial dilution starting at 20 μM. Reactions were carried out at 10 μM ATP. IC_{50} values were calculated using Prism 7.0 (GraphPad).[45]

RPPA (reverse phase protein array). RPPA analysis was performed by MD Anderson Cancer Center RPPA core facility. MDA-MB-231 cells were grown in complete growth medium. Cells were treated for 24 h with **PROTAC-3** (500 nM), defactinib (1 μM) or DMSO (0.1%), trypsinized and allowed to reattach for 8 h in the presence of compound or DMSO before cells were subjected to lysis and samples prepared according to protocols provided by MD Anderson.

Wound healing assay. MDA-MB-231 cells were maintained in complete growth medium at 37 °C supplied with 5% CO_2. Cells ($1x10^6$) were split in to a 12-well plate. After 24 h an even wound was created across each well using a sterile 10 μL pipette tip and the cells were with washed warm PBS twice to remove any floating or dead cells. This time point was considered as 0 h and cells were incubated in fresh medium containing PROTAC or control as indicated for 24 h. Images of wounded area were captured at 0 h and after 24 h using a camera attached to a light microscope. Images were analyzed by ImageJ software and wounded area was quantified. The area of the remaining wound at 24 h was subtracted from the area of the wound at 0 h. Percent wound healing (migration) was calculated and data presented as a bar graph using Prism 7.0 (GraphPad).[45] Differences between groups were analyzed by Welch's t-test and considered significant when $p<0.05$.

Transwell invasion assay. On the first day, 0.2x Basement Membrane Extract (BME) working solution was prepared by diluting 5x BME stock solution in 1x Travigen Inc. coating buffer. Briefly, 100 μL of 10x coating buffer was diluted in 900 μL of sterile water to make 1x coating buffer. Then 960 μL of 1x coating buffer was mixed with 40 μL of 5x BME to make working 0.2x BME solution. Corning Transwell permeable inserts (Costar Transwell chambers, Corning) were placed on a 24-well plate and 100 μL of 0.2x BME solution was added to each Transwell insert and incubated for 16 h. Following day, MDA-MB-231 cells were trypsinized and cells were suspended in serum free medium. Approximately 100 μL from cell suspension (~$3x10^5$ cells) was added to each Transwell insert followed by another 100 μL of PROTAC or control containing serum free RPMI medium. The lower chamber was filled with 10% FBS containing RPMI medium and the whole setup was incubated at 37 °C, 5% CO_2 for 24 h. After 24 h, cell culture medium was removed from both lower and upper chambers and Transwell inserts were washed three times

with PBS. Non-invasive cells were removed using a cotton swab and bottom side of the membrane of Transwell inserts were fixed with 4% formaldehyde for 10 min at room temperature followed by permeabilization with PBST (pH-7.4, 50 mM Tris-HCl, 150 mM NaCl, 0.1% Triton-X100) for another 10 min. Inserts were washed once with PBS and stained with 0.2% (W/V) crystal violet solution for 20 min at room temperature. Inserts were then extensively washed with PBS and once with water to remove all excess dye and salts. Cells migrated through the membrane were captured using a camera attached to a light microscope. Images were then analyzed by ImageJ software and number of cells on the bottom side of the membrane were counted and presented as a bar graph using Prism 7.0 (GraphPad).[45] Differences among groups were analyzed by Welch's t-test and considered significant when $P < 0.05$.

Acknowledgements

P.M.C. is thankful to the Alexander von Humboldt Foundation for a Feodor Lynen research fellowship. J.H. is generously supported by a National Cancer Institute specialist award (R50CA211252). C.M.C. gratefully acknowledges the US National Institutes of Health for their support (R35CA197589).

Financial Disclosure

C.M.C. is founder, shareholder, and consultant to Arvinas, LLC. In addition, his lab receives sponsored research support from Arvinas.

References

(1) Lee, B. Y.; Timpson, P.; Horvath, L. G.; Daly, R. J. FAK signaling in human cancer as a target for therapeutics. *Pharmacol. Ther.* **2015**, *146*, 132–149.

(2) Sulzmaier, F. J.; Jean, C.; Schlaepfer, D. D. FAK in cancer: mechanistic findings and clinical applications. *Nat. Rev. Cancer* **2014**, *14*, 598–610.

(3) Cance, W. G.; Kurenova, E.; Marlowe, T.; Golubovskaya, V. Disrupting the scaffold to improve focal adhesion kinase-targeted cancer therapeutics. *Sci. Signal* **2013**, *6*, pe10.

(4) Schaller, M. D. Cellular functions of FAK kinases: insight into molecular mechanisms and novel functions. *J. Cell. Sci.* **2010**, *123*, 1007–1013.

(5) Mitra, S. K.; Hanson, D. A.; Schlaepfer, D. D. Focal adhesion kinase: in command and control of cell motility. *Nat. Rev. Mol. Cell Biol.,* **2005**, *6*, 56–68.

(6) Frame, M. C.; Patel, H.; Serrels, B.; Lietha, D.; Eck, M. J. The FERM domain: organizing the structure and function of FAK. *Nat. Rev. Mol. Cell Biol.* **2010**, *11*, 802–814.

(7) Pylayeva, Y.; Gillen, K. M.; Gerald, W.; Beggs, H. E.; Reichardt, L. F.; Giancotti, F. G. Ras- and PI3K-dependent breast tumorigenesis in mice and humans requires focal adhesion kinase signaling. *J. Clin. Invest.* **2009**, *119*, 252–266.

(8) Serrels, A.; Lund, T.; Serrels, B.; Byron, A.; McPherson, R. C.; Kriegsheim, A. von; Gómez-Cuadrado, L.; Canel, M.; Muir, M.; Ring, J. E.; Maniati, E.; Sims, A. H.; Pachter, J. A.; Brunton, V. G.; Gilbert, N.; Anderton, S. M.; Nibbs, R. J. B.; Frame, M. C. Nuclear FAK controls chemokine transcription, Tregs, and evasion of anti-tumor immunity. *Cell* **2015**, *163*, 160–173.

(9) Jiang, H.; Hegde, S.; Knolhoff, B. L.; Zhu, Y.; Herndon, J. M.; Meyer, M. A.; Nywening, T. M.; Hawkins, W. G.; Shapiro, I. M.; Weaver, D. T.; Pachter, J. A.; Wang-Gillam, A.; DeNardo, D. G. Targeting focal adhesion kinase renders pancreatic cancers responsive to checkpoint immunotherapy. *Nat. Med.* **2016**, *22*, 851–860.

(10) Ott, G. R.; Cheng, M.; Learn, K. S.; Wagner, J.; Gingrich, D. E.; Lisko, J. G.; Curry, M.; Mesaros, E. F.; Ghose, A. K.; Quail, M. R.; Wan, W.; Lu, L.; Dobrzanski, P.; Albom, M. S.; Angeles, T. S.; Wells-Knecht, K.; Huang, Z.; Aimone, L. D.; Bruckheimer, E.; Anderson, N.; Friedman, J.; Fernandez, S. V.; Ator, M. A.; Ruggeri, B. A.; Dorsey, B. D. Discovery of Clinical Candidate CEP-37440, a Selective Inhibitor of Focal Adhesion Kinase (FAK) and Anaplastic Lymphoma Kinase (ALK). *J. Med. Chem.* **2016**, *59*, 7478–7496.

(11) Beraud, C.; Dormoy, V.; Danilin, S.; Lindner, V.; Bethry, A.; Hochane, M.; Coquard, C.; Barthelmebs, M.; Jacqmin, D.; Lang, H.; Massfelder, T. Targeting FAK scaffold functions inhibits human renal cell carcinoma growth. *Int J Cancer* **2015**, *137*, 1549–1559.

(12) Fan, H.; Zhao, X.; Sun, S.; Luo, M.; Guan, J.-L. Function of focal adhesion kinase scaffolding to mediate endophilin A2 phosphorylation promotes epithelial-mesenchymal transition and mammary cancer stem cell activities in vivo. *J. Biol. Chem.* **2013**, *288*, 3322–3333.

(13) Burslem, G. M.; Crews, C. M. Small-Molecule Modulation of Protein Homeostasis. *Chem. Rev.* **2017**, *117*, 11269–11301.

(14) Cromm, P. M.; Crews, C. M. Targeted Protein Degradation: From Chemical Biology to Drug Discovery. *Cell Chem. Biol.* **2017**, *24*, p1181–1190.

(15) Ottis, P.; Crews, C. M. Proteolysis-Targeting Chimeras: Induced Protein Degradation as a Therapeutic Strategy. *ACS Chem. Biol.* **2017**, *12*, 892–898.

(16) Sakamoto, K. M.; Kim, K. B.; Kumagai, A.; Mercurio, F.; Crews, C. M.; Deshaies, R. J. Protacs: chimeric molecules that target proteins to the Skp1-Cullin-F box complex for ubiquitination and degradation. *Proc. Natl. Acad. Sci. U.S.A.* **2001**, *98*, 8554–8559.

(17) Schneekloth, J. S., JR; Fonseca, F. N.; Koldobskiy, M.; Mandal, A.; Deshaies, R.; Sakamoto, K.; Crews, C. M. Chemical genetic control of protein levels: selective in vivo targeted degradation. *J. Am. Chem. Soc.* **2004**, *126*, 3748–3754.

(18) Schneekloth, A. R.; Pucheault, M.; Tae, H. S.; Crews, C. M. Targeted intracellular protein degradation induced by a small molecule: En route to chemical proteomics. *Bioorg. Med. Chem. Lett.* **2008**, *18*, 5904–5908.

(19) Itoh, Y.; Ishikawa, M.; Naito, M.; Hashimoto, Y. Protein knockdown using methyl bestatin-ligand hybrid molecules: design and synthesis of inducers of ubiquitination-mediated degradation of cellular retinoic acid-binding proteins. *J. Am. Chem. Soc.* **2010**, *132*, 5820–5826.

(20) Itoh, Y.; Ishikawa, M.; Kitaguchi, R.; Sato, S.; Naito, M.; Hashimoto, Y. Development of target protein-selective degradation inducer for protein knockdown. *Bioorg. Med. Chem.* **2011**, *19*, 3229–3241.

(21) Bondeson, D. P.; Mares, A.; Smith, I. E. D.; Ko, E.; Campos, S.; Miah, A. H.; Mulholland, K. E.; Routly, N.; Buckley, D. L.; Gustafson, J. L.; Zinn, N.; Grandi, P.; Shimamura, S.; Bergamini, G.; Faelth-Savitski, M.; Bantscheff, M.; Cox, C.; Gordon, D. A.; Willard, R. R.; Flanagan, J. J.; Casillas, L. N.; Votta, B. J.; den Besten, W.; Famm, K.; Kruidenier, L.; Carter, P. S.; Harling, J. D.; Churcher, I.; Crews, C. M. Catalytic in vivo protein knockdown by small-molecule PROTACs. *Nat. Chem. Biol.* **2015**, *11*, 611–617.

(22) Winter, G. E.; Buckley, D. L.; Paulk, J.; Roberts, J. M.; Souza, A.; Dhe-Paganon, S.; Bradner, J. E. Phthalimide conjugation as a strategy for in vivo target protein degradation. *Science* **2015**, *348*, 1376–1381.

(23) Lu, J.; Qian, Y.; Altieri, M.; Dong, H.; Wang, J.; Raina, K.; Hines, J.; Winkler, J. D.; Crew, A. P.; Coleman, K.; Crews, C. M. Hijacking the E3 Ubiquitin Ligase Cereblon to Efficiently Target BRD4. *Chem. Biol.* **2015**, *22*, 755–763.

(24) Zengerle, M.; Chan, K.-H.; Ciulli, A. Selective Small Molecule Induced Degradation of the BET Bromodomain Protein BRD4. *ACS Chem. Biol.* **2015**, *10*, 1770–1777.

(25) Huang, H.-T.; Dobrovolsky, D.; Paulk, J.; Yang, G.; Weisberg, E. L.; Doctor, Z. M.; Buckley, D. L.; Cho, J.-H.; Ko, E.; Jang, J.; Shi, K.; Choi, H. G.; Griffin, J. D.; Li, Y.; Treon, S. P.; Fischer, E. S.; Bradner, J. E.; Tan, L.; Gray, N. S. A Chemoproteomic Approach to Query the Degradable Kinome Using a Multi-kinase Degrader. *Cell Chem. Biol.* **2018**, *25*, 88-99.e6.

(26) Galdeano, C.; Gadd, M. S.; Soares, P.; Scaffidi, S.; van Molle, I.; Birced, I.; Hewitt, S.; Dias, D. M.; Ciulli, A. Structure-guided design and optimization of small molecules targeting the protein-protein interaction between the von Hippel-Lindau (VHL) E3 ubiquitin ligase and the hypoxia inducible factor (HIF) alpha subunit with in vitro nanomolar affinities. *J. Med. Chem.* **2014**, *57*, 8657–8663.

(27) Buckley, D. L.; Gustafson, J. L.; van Molle, I.; Roth, A. G.; Tae, H. S.; Gareiss, P. C.; Jorgensen, W. L.; Ciulli, A.; Crews, C. M. Small-molecule inhibitors of the interaction between the E3 ligase VHL and HIF1alpha. *Angew. Chem. Int. Ed.* **2012**, *51*, 11463–11467.

(28) Buckley, D. L.; van Molle, I.; Gareiss, P. C.; Tae, H. S.; Michel, J.; Noblin, D. J.; Jorgensen, W. L.; Ciulli, A.; Crews, C. M. Targeting the von Hippel-Lindau E3 ubiquitin ligase using small molecules to disrupt the VHL/HIF-1alpha interaction. *J. Am. Chem. Soc.* **2012**, *134*, 4465–4468.

(29) Luzzio, M. J.; Autry, C. L.; Bhattacharya, S. K.; Freeman-Cook, K. D.; Hayward, M. M.; Hulford, C. A.; Nelson, K. L.; Xiao, J.; Zhao, X. *Sulfonyl amide derivatives for the treatment of abnormal cell growth*; WO Patent, 2008 (WO2008/129380).

(30) Bondeson, D. P.; Smith, B. E.; Burslem, G. M.; Buhimschi, A. D.; Hines, J.; Jaime-Figueroa, S.; Wang, J.; Hamman, B. D.; Ishchenko, A.; Crews, C. M. Lessons in PROTAC Design from Selective Degradation with a Promiscuous Warhead. *Cell Chem. Biol.* **2018**, *25*, p78–87.

(31) Lee, Y.-C.; Lin, S.-C.; Yu, G.; Cheng, C.-J.; Liu, B.; Liu, H.-C.; Hawke, D. H.; Parikh, N. U.; Varkaris, A.; Corn, P.; Logothetis, C.; Satcher, R. L.; Yu-Lee, L.-Y.; Gallick, G. E.; Lin, S.-H. Identification of Bone-Derived Factors Conferring De Novo Therapeutic Resistance in Metastatic Prostate Cancer. *Cancer Res.* **2015**, *75*, 4949–4959.

(32) Douglass, E. F.; Miller, C. J.; Sparer, G.; Shapiro, H.; Spiegel, D. A. A comprehensive mathematical model for three-body binding equilibria. *J. Am. Chem. Soc.* **2013**, *135*, 6092–6099.

(33) Lahlou, H.; Sanguin-Gendreau, V.; Frame, M. C.; Muller, W. J. Focal adhesion kinase contributes to proliferative potential of ErbB2 mammary tumour cells but is dispensable for ErbB2 mammary tumour induction in vivo. *Breast Cancer Res* **2012**, *14*, R36.

(34) Castoria, G.; D'Amato, L.; Ciociola, A.; Giovannelli, P.; Giraldi, T.; Sepe, L.; Paolella, G.; Barone, M. V.; Migliaccio, A.; Auricchio, F. Androgen-Induced Cell Migration: Role of Androgen Receptor/Filamin A Association. *PLoS ONE* **2011**, *6*, e17218.

(35) Castoria, G.; Auricchio, F.; Migliaccio, A. Extranuclear partners of androgen receptor: at the crossroads of proliferation, migration, and neuritogenesis. *FASEB J.* **2017**, *31*, 1289–1300.

(36) Hutchinson, J. A.; Shanware, N. P.; Chang, H.; Tibbetts, R. S. Regulation of Ribosomal Protein S6 Phosphorylation by Casein Kinase 1 and Protein Phosphatase 1. *J. Biol. Chem.* **2011**, *286*, 8688–8696.

(37) Lepin, E. J.; Zhang, Q.; Zhang, X.; Jindra, P. T.; Hong, L. S.; Ayele, P.; Peralta, M. V. P.; Gjertson, D. W.; Kobashigawa, J. A.; Wallace, W. D.; Fishbein, M. C.; Reed, E. F. Phosphorylated S6 Ribosomal Protein: A Novel Biomarker of Antibody-Mediated Rejection in Heart Allografts. *Am J Transplant* **2006**, *6*, 1560–1571.

(38) Valeur, E.; Jimonet, P. New Modalities, Technologies, and Partnerships in Probe and Lead Generation: Enabling a Mode-of-Action Centric Paradigm. *J. Med. Chem.* **2018**, DOI: 10.1021/acs.jmedchem.8b00378.

(39) Waldmann, H.; Valeur, E.; Guéret, S. M.; Adihou, H.; Gopalakrishnan, R.; Lemurell, M.; Grossmann, T. N.; Plowright, A. T. New Modalities for Challenging Targets in Drug Discovery. *Angew. Chem. Int. Ed.* **2017**, *56*, 10294–10323.

(40) Cromm, P. M.; Spiegel, J.; Grossmann, T. N. Hydrocarbon Stapled Peptides as Modulators of Biological Function. *ACS Chem. Biol.* **2015**, *10*, 1362–1375.

(41) Spiegel, J.; Cromm, P. M.; Zimmermann, G.; Grossmann, T. N.; Waldmann, H. Small-molecule modulation of Ras signaling. *Nat. Chem. Biol.* **2014**, *10*, 613–622.

(42) Cromm, P. M.; Spiegel, J.; Grossmann, T. N.; Waldmann, H. Direct Modulation of Small GTPase Activity and Function. *Angew. Chem. Int. Ed.* **2015**, *54*, 13516–13537.

(43) Ferguson, F. M.; Gray, N. S. Kinase inhibitors: the road ahead. *Nat. Rev. Drug Discov.* **2018**, *17*, 353–377.

(44) Jones, L. H. Small-Molecule Kinase Downregulators. *Cell Chem. Biol.* **2018**, *25*, 30–35.

(45) Motulsky, H.; Christopoulos, A. *Fitting models to biological data using linear and nonlinear regression: A practical guide to curve fitting*; Oxford University Press: Oxford, New York, 2004.